The role of dislocation mobility on the hydrogen induced mechanical degradation of Fe-C-X alloys

Tom DEPOVER, Kim VERBEKEN

Ghent University, Zwijnaarde, Belgium, tom.depover@ugent.be
Ghent University, Zwijnaarde, Belgium, kim.verbeken@ugent.be

Abstract:
Due to the estimated increase in population, the limited fossil resources, the concerns about nuclear energy and above all the global warming issues, scientists are triggered to come up with solutions. One of the suggested replacements for fossil fuels is hydrogen gas. However, the presence of hydrogen in metals is known to be detrimental for the overall performance and more specific the ductility of the materials. Unpredictable failure still occurs and although decades of research have been performed, still open questions remain. During the recent developments of material's design, precipitates play an important role since they can strengthen the material and enhance the resistance against this hydrogen induced failure. Well-designed hydrogen trapping sites might be a relevant strategy to enhance the resistance to hydrogen embrittlement.

The present work considers four types of carbides in three Fe-C-X alloys with increasing carbon content: Ti, Cr, Mo and V-based precipitates. Two conditions were compared for each composition to evaluate the effect of these precipitates: as quenched and quenched and tempered, carbides were introduced during tempering. The material/hydrogen interaction was fully characterized. In-situ tensile tests were performed to evaluate the sensitivity to hydrogen embrittlement. Thermal desorption spectroscopy was done to evaluate the hydrogen trapping capacity of the precipitates, whereas hot/melt extraction was performed to determine the hydrogen content. All tests were done after hydrogen pre-charging till saturation.

The degree of hydrogen embrittlement was correlated with the amount of hydrogen present in the alloys. Three different types of hydrogen, determined by the strength by which they were trapped, were analyzed by combining the different hydrogen characterization techniques. It was established that hydrogen trapped at dislocations played a determinant role. This further confirmed the importance of an enhanced dislocation mobility in the presence of hydrogen, which is a solid experimental proof of the HELP mechanism. On the contrary, hydrogen trapped by the precipitates did not show a considerable impact of the hydrogen induced mechanical degradation. For all carbides, the addition was beneficial to enhance the resistance since they were able to deeply trap a significant amount of hydrogen.

Keywords: hydrogen induced mechanical degradation; hydrogen trapping; hydrogen dislocation mobility; HELP; carbides

Introduction

The detrimental effect of hydrogen (H) on the mechanical properties of steel has been reported to impede the development of high strength steels [1]. Although the H induced damage was already discussed in 1875 by Johnson [2], no complete understanding of the phenomenon has been obtained so far. Several mechanisms have been proposed to describe the occurrence, but none has been solely accepted since multiple indications linked to the different mechanisms have been observed or experimental evidence is lacking. The three most cited mechanisms are the Hydrogen Enhanced DEcohesion (HEDE) [3], the Hydrogen Enhanced Localized Plasticity (HELP) [4] and Adsorption Induced Dislocation Emission (AIDE) theory [5].

A relevant topic in steel alloy development has been the role of carbides [6], since they, on the one hand, induce material strenghtening due to precipitation hardening and, on the other hand, are often mentioned to be beneficial as efficient deep H trapping sites. As such, H is avoided to get trapped as highly diffusible H since this type is assumed to be the most detrimental one. Even though thermal desorption spectroscopy (TDS) studies revealed the H trapping capacity of numerous precipitates [7-14], literature relating their effect to the mechanical behavior in the presence of H is limited [15, 16].

However, steels with an increased strength level are considered to be more prone to H induced mechanical degradation [17-19]. The interaction of these high strength steels with H has been considered thoroughly during the last decade [20-22]. Recently, the research group on H at Ghent University has presented results on four industrial multiphase high strength steels, i.e. dual phase (DP), transformation induced plasticity (TRIP), ferrite-bainite (FB) and high strength low alloy steel (HSLA) [23-28]. The impact of H on the mechanical properties was specifically studied in [19] and a significant H induced ductility loss was observed, except for the HSLA steel, which was attributed to the presence of Ti- and Nb- carbo-nitrides.

More emphasis has been put on the addition of carbides as effective H trapping sites to enhance the susceptibility to H induced material degradation. Trapping diffusible H using nano-sized carbides as H traps is generally assumed to be one of the main strategies to enhance the resistance against hydrogen embrittlement (HE) [15, 19, 29]. However, the complex microstructure of multiphase steels obstructs interpreting H related findings. Therefore, specifically designed Fe-C-X alloys were recently investigated by our H-group as well. Carbide forming elements, i.e. X = Ti, Cr, Mo and V, were added as ternary alloying element [30-33]. Results on each Fe-C-X grade were published separately focusing on one specific type of carbide forming element to fully comprehend the underlying mechanism taking place for each considered precipitate. The present study however aims to compare the different carbides to draw general conclusions in terms of their effect on the H induced mechanical degradation.

Experimental procedure

Four different Fe-C-X grades with a stoichiometric amount of a ternary alloying element X were processed. Each grade was incrementally cast into three alloys with increasing carbon content (cf. Table 1). The carbon increase allows a reliable assessment of the effect of the carbides with varying strength level and moreover a confirmation regarding their role in different alloys. The Fe-C-X materials were cast, hot rolled and subsequently austenitized at 1250°C for 10 minutes followed by a brine water quench. This first condition will be referred

to as “as-Q”. Furthermore, also a tempering treatment of 1h was applied to introduce small carbides in this martensitic microstructure. Secondary hardening due to the precipitation of carbides was optimal at 600°C for the Fe-C-Ti, Fe-C-Mo and Fe-C-V alloys and at 550°C for the Fe-C-Cr material. The hardness profiles versus tempering temperature can be found elsewhere [30-33]. This second condition will be referred to as “Q&T”. The microstructures were studied by optical microscopy, scanning electron microscopy and transmission electron microscopy (TEM) and the degree of H induced mechanical degradation, the H content and TDS measurements were determined as described in detail in [30-33]. Alloy B of each Fe-C-X cast will be discussed in depth for this comparative study. For the experimental data on alloy A and C, we wish to refer the reader to the corresponding publications [30-33].

Table 1: *Chemical compositions of the Fe-C-X materials.*

Alloy Fe-C-X		**wt.% C**	**wt.% X**	**Other elements**
Fe-C-Ti	Alloy A	0.099	0.380	Al: 200-300 wt. ppm Other elements: traces
	Alloy B	0.202	0.740	
	Alloy C	0.313	1.340	
Fe-C-Cr	Alloy A	0.097	1.300	
	Alloy B	0.143	1.800	
	Alloy C	0.184	2.200	
Fe-C-Mo	Alloy A	0.100	1.700	
	Alloy B	0.142	2.380	
	Alloy C	0.177	2.990	
Fe-C-V	Alloy A	0.100	0.570	
	Alloy B	0.190	1.090	
	Alloy C	0.286	1.670	

The H/material interaction tests were done on H saturated samples by pre-charging the materials in a 1g/L thiourea in a 0.5 M H_2SO_4 solution at a current density of 0.8 mA/cm^2 for 1 hour. Hot/melt extraction was performed to determine the H content. The samples were analysed about one minute after H charging and the measurements were done at 1600°C and 300°C to determine the total and diffusible H content. TDS was done to identify both the H trapping sites and their corresponding activation energy. Therefore, three different heating rates were used (200°C/h, 600°C/h and 1200°C/h). The applied procedure required one hour between the end of H charging and the start of the TDS measurement as a sufficient vacuum needs to be created in the analysis chamber. The effect of H release during this time will be further discussed. The degree of H induced mechanical degradation was determined as:

$$\%HE = 100 \cdot \left(1 - \frac{\varepsilon_{ch}}{\varepsilon_{un}}\right)$$

with ε_{ch} and ε_{un} being the elongation of the H charged and uncharged tensile sample, respectively. Hence, the %HE varies between 0 and 1, with 0 meaning that there is no ductility loss and the material is insensitive to HE. When an index of 1 is obtained, the ductility drop is 100% and HE is maximal.

Materials characterization

Optical microscopy showed a clear martensitic and Q&T microstructure. The as-Q condition of grade Fe-C-Ti alloy B showed still large incoherent carbides since austenitizing at 1250°C was not sufficient to dissolve all the present carbides after casting and rolling (cf. Fig. 1 and Fig. 2 (a)). For the other grades (Fe-C-Cr, -Mo and –V), all the carbides were dissolved as illustrated in Fig. 1, which is based on the thermodynamical calculations to determine the

amount of dissolved carbon. Precipitates were introduced during the tempering treatment for the Q&T condition. TEM bright field images were taken to confirm their presence as presented in Fig. 2 (b-e). Small carbides with sizes less than 10 nm were displayed for the Ti- and V-alloy while coarser precipitates were detected for the Mo- and Cr-alloy. Only the as-Q condition of Fe-C-Ti alloy B contained undissolved incoherent TiC (cf. Fig. 2 (a)). More microstructural details and diffraction patterns for identification of the different carbides (TiC, $Cr_{23}C_6$, Mo_2C and V_4C_3) can be found in the corresponding publications [30-33].

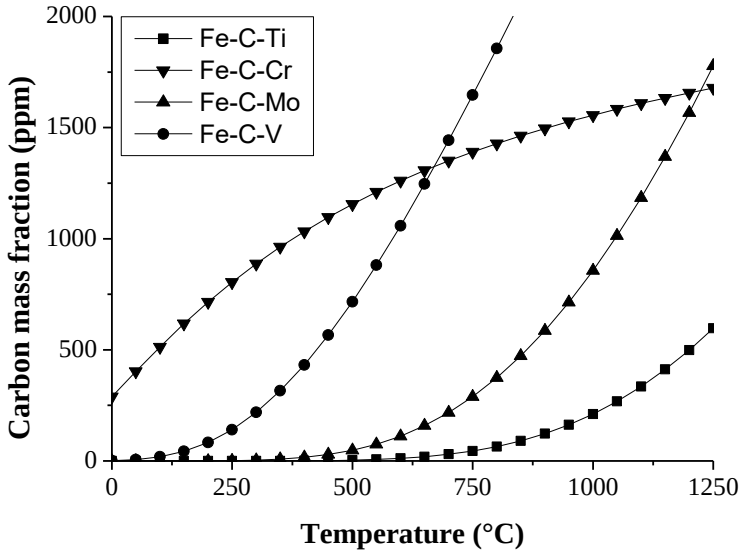

Fig. 1*: Mass fraction of carbon (ppm) vs. temperature (°C) that can be kept in solid solution at each temperature for stoichiometric total contents of C and Ti, Cr, Mo or V.*

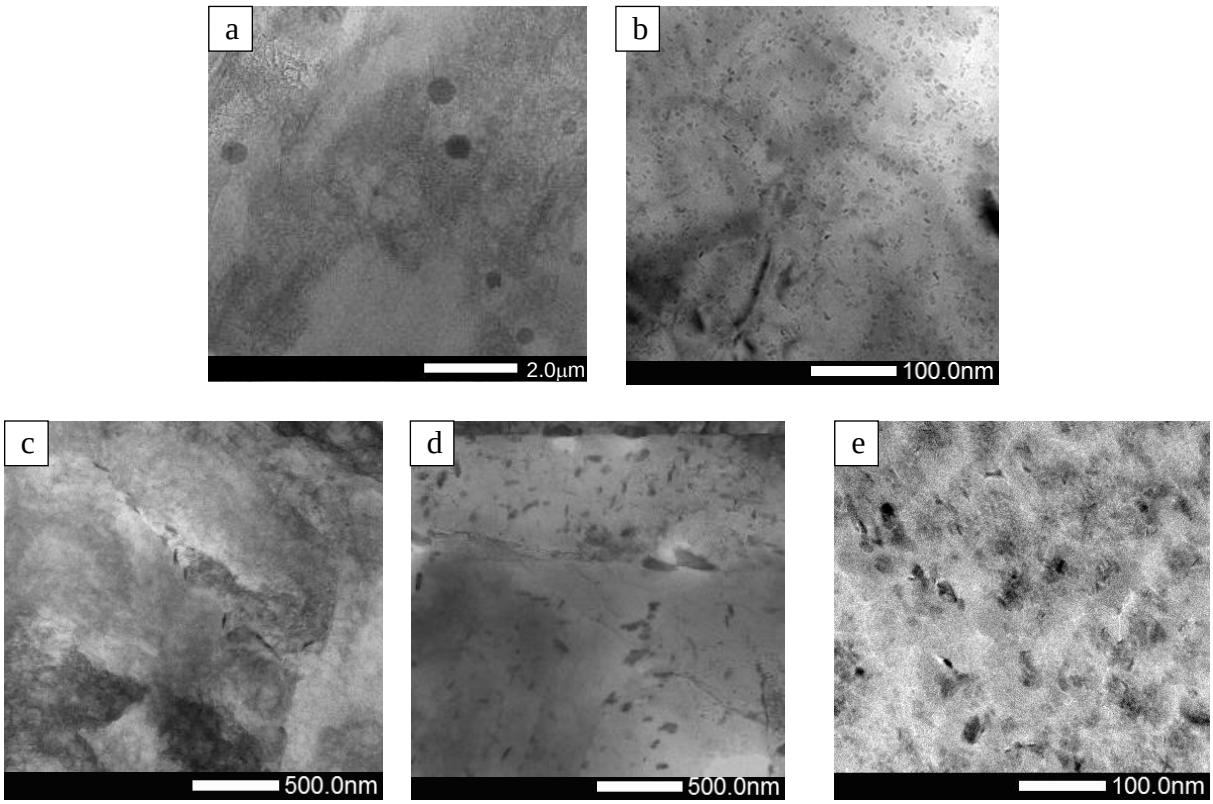

Fig. 2*: TEM bright field images for Fe-C-Ti in the as-Q condition (a) and for Fe-C-Ti (b), Fe-C-Cr (c), Fe-C-Mo (d) and Fe-C-V (e) in the Q&T condition.*

Hydrogen induced mechanical degradation

The stress-strain curves for Ti-, Cr-, Mo- and V-alloy B in the as-Q and Q&T condition are depicted in Fig. 3. A significantly different HE susceptibility was observed for the four alloys. Tempering resulted in an increase in strength level and ductility for the Fe-C-Ti and Fe-C-Mo alloy, while a reduction for both was observed for the Fe-C-Cr alloy due the presence of coarse particles. A similar observation was made for Fe-C-V although limited plastic deformation took place since carbides dissolved fast during austenitizing resulting in a dense carbon rich martensitic microstructure and a more brittle material (cf. Fig. 1). The degree of HE increased when comparing the as-Q with the Q&T condition for Fe-C-Ti (21 – 60%), Fe-C-Mo (13 – 23%) and Fe-C-V (28 – 32%), while a decrease was detected for Fe-C-Cr (39 – 21%). To understand these results, the H/material interaction was studied in much detail.

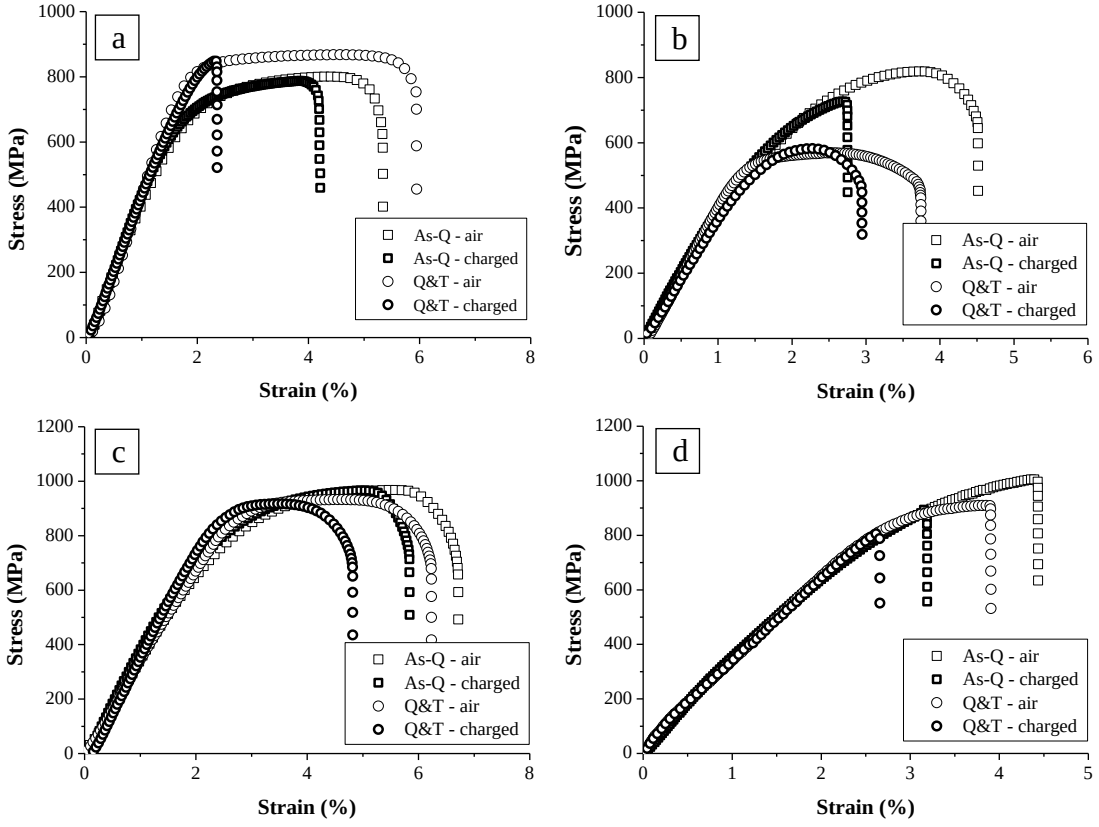

Fig. 3: *Stress-strain curves for (a) Fe-C-Ti, (b) Fe-C-Cr, (c) Fe-C-Mo and (d) Fe-C-V alloy B at a cross-head deformation speed of 5 mm/min of uncharged (air) and H saturated (charged) samples.*

Hydrogen/material interaction

TDS was performed on all Fe-C-X grades in both the as-Q and Q&T condition as summarized in Fig. 4. Basically, the first peak was correlated to H trapped by lath boundaries, while the other peaks were linked to H trapped by the carbides. Only one peak was observed for the as-Q conditions, indicating that the incoherent large TiC particles (cf. Fig 2(a)) were not able to trap H from electrochemical charging. This confirmed previous results; gaseous H charging at elevated temperature is required to charge these large particles [11, 12]. When considering the Q&T condition, additional peaks can be detected linked to the presence of tempered induced carbides. Especially the small TiC and V_4C_3 carbides were capable of trapping a lot of H, while the coarser $Cr_{23}C_6$ and Mo_2C only showed a small peak correlated to H trapped by these

carbides. A more detailed interpretation of these data including activation energies of the deconvoluted peaks can be found elsewhere [30-33].

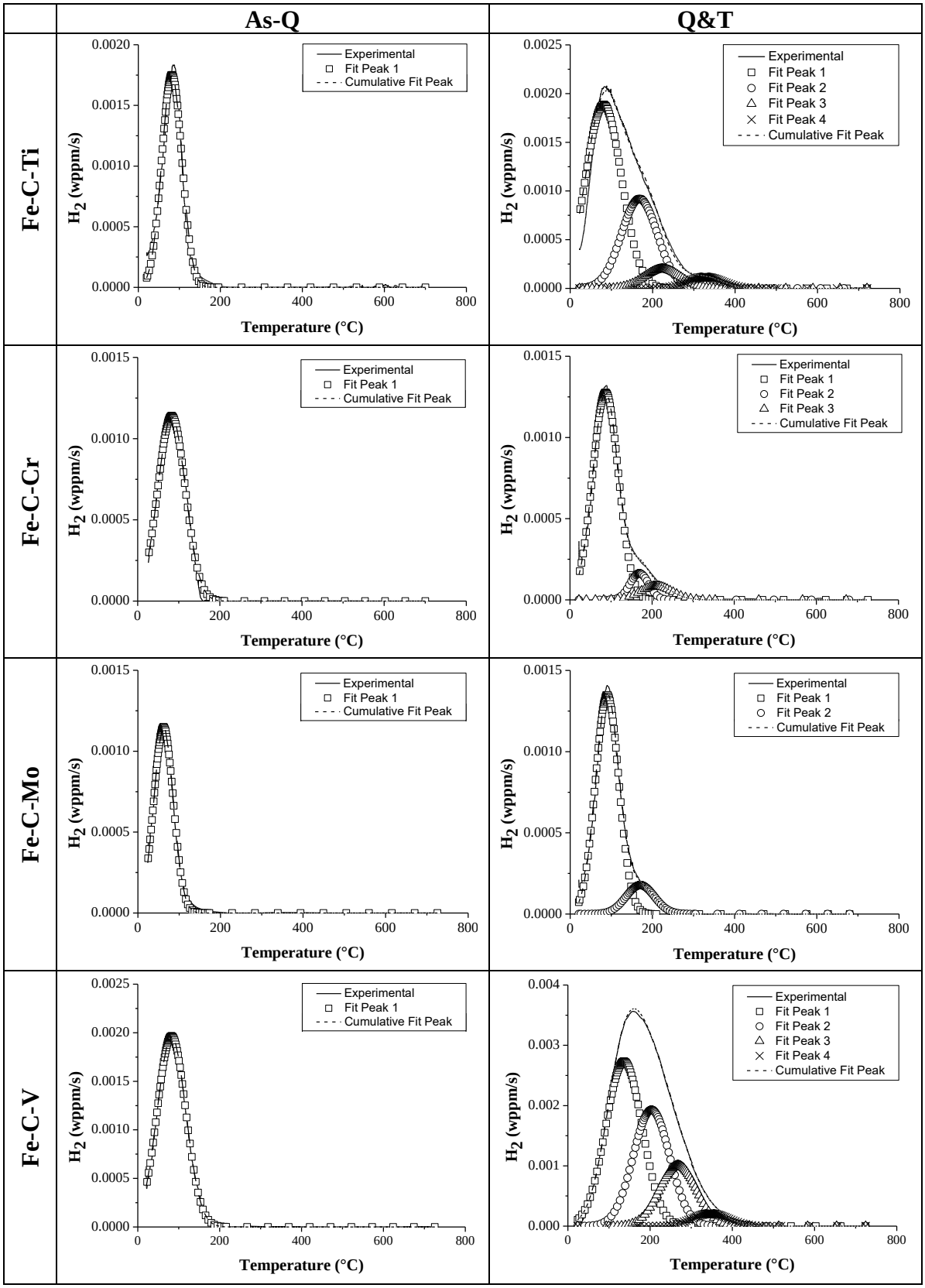

Fig. 4: *TDS curves of Fe-C-X grades (alloy B) in the as-Q and Q&T condition (heating rate: 600°C/h).*

Hot (at 300°C) and melt (at 1600°C) extraction, which provides the diffusible and total H content of the H saturated samples, was performed (cf. Fig. 5). For the Fe-C-Ti and Fe-C-V materials, the diffusible and total H content clearly increased when the sample was tempered. Consequently, the microstructural changes that occurred during tempering, mainly the formation of a considerable amount of small Ti or V-carbides, provided an important increase in H trapping sites in the material (as experimentally confirmed by the TDS results). The Mo- and Cr-alloys showed a significantly lower H content, while the amount of diffusible H was the lowest for the Fe-C-Mo alloy. Moreover, the difference between as-Q and Q&T was also rather small, especially for Fe-C-Cr. Although tempering induced significant microstructural changes as well and therefore, also in the potential trapping sites, the H trapping capacity of both conditions appeared to be similar.

There is a clear difference between the amount of H as determined by hot extraction, i.e. diffusible H, and the total area below the TDS curve. Indeed, H was able leave the sample before the TDS measurement, as it took about 1 h to reach a sufficiently low vacuum in the TDS chamber (cf. experimental procedure). This type of H will be defined as "mobile H" [30-33]. As demonstrated [25], microstructural defects such as dislocations indeed trap H, but loose it before the measurement started. During the in-situ tensile tests, however, this mobile H is still present and very relevant for the obtained results as discussed below. An overview of the H contents is summarized in Fig. 5.

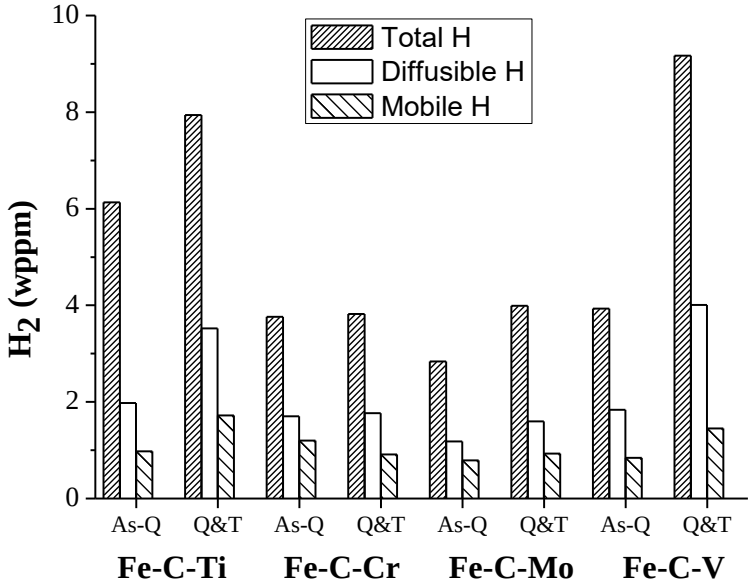

Fig. 5: *The total, diffusible and mobile H contents of the Fe-C-X grades (alloy B) in the as-Q and Q&T condition.*

The HE degree for the Fe-C-Ti alloy in the Q&T condition was higher compared to the as-Q state due to the higher amount of H. This could be attributed to the TiC precipitates formed during tempering, which not only increased the H trapping capacity as compared to the as-Q samples, but also introduced weakly trapped H at the elastic stress fields in the matrix surrounding the particle [11, 32]. The as-Q Cr-alloy embrittled more than the Q&T material although similar amounts of total and diffusible H were measured. However, due to the trapping ability of the carbides in the Q&T state (cf. TDS data), more mobile H was present in the as-Q material. Consequently, the Q&T alloy showed a lower susceptibility to HE [30]. The Fe-C-Mo alloys showed a decreased resistance against H induced failure when tempered induced carbides were present. This can be correlated to higher amounts of H detected in the Q&T samples. Finally, the Fe-C-V alloys exposed rather low strain levels and the H charged

specimen broke on the edge of the elastic/plastic region of the stress-strain curve. However, tempering even increased the sensitivity to HE due to the higher amount of H, trapped by the V-carbides. Since hardly any plastic deformation occurred for these alloys, the effect of mobile H, trapped at dislocations, is assumed to be minimal [33], as discussed below.

To further analyse the hypothesis on the correlation between the HE degree and the amount of mobile H, the relation between the different types of H (i.e. total, diffusible and mobile) and HE is plotted together with a linear fitting (cf. Fig. 6 (a)). This was done for alloy A, B and C for each Fe-C-X grade in the as-Q and Q&T condition (24 materials). The correlation improves for total over diffusible to mobile H. Moreover, when the Fe-C-V materials were excluded (cf. Fig. 6 (b)), a R^2 of 96% between the HE% and the amount of mobile H was obtained. This indicated the crucial importance of the amount of H trapped by dislocations and the enhancement of the dislocation mobility by the presence of H as proposed by the HELP mechanism.

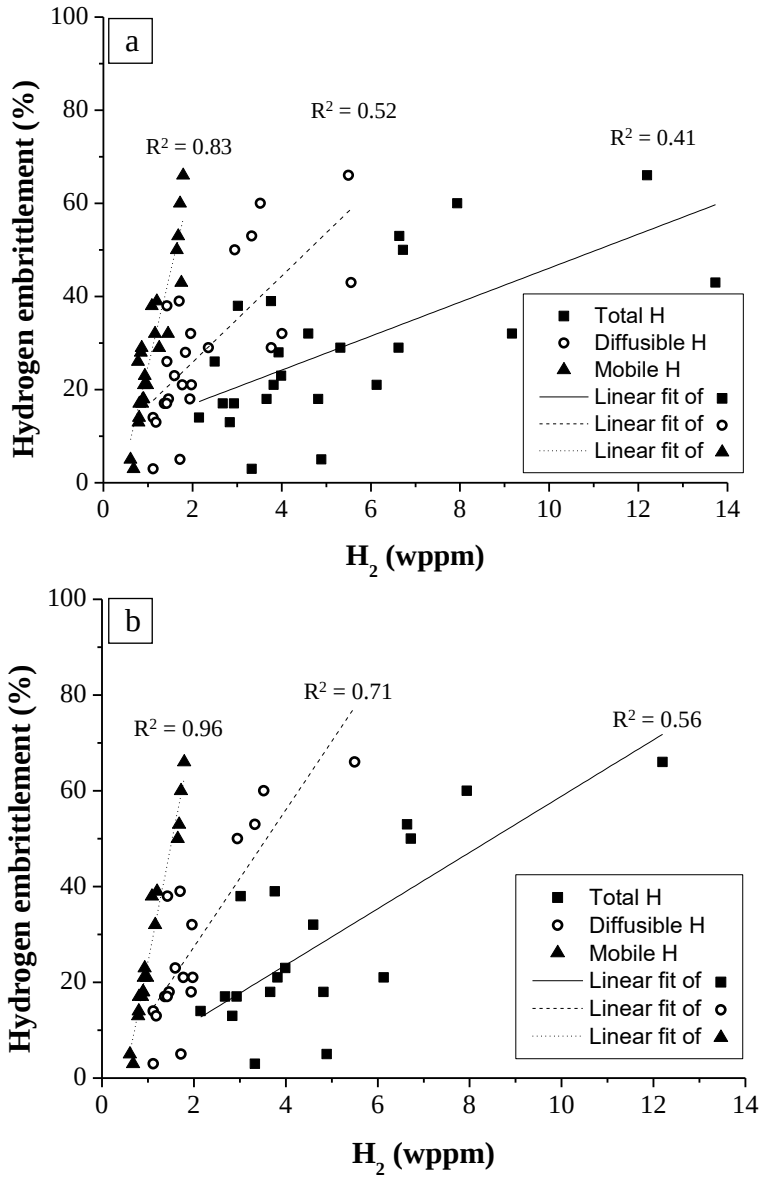

Fig. 6: *Degree of HE vs. the total, diffusible and mobile H content for Fe-C-X grade – alloy A, B and C in the as-Q and Q&T condition (a). The Fe-C-V alloys were excluded in (b) to illustrate very nicely the correlation between mobile H and HE for alloys which failed past the macroscopic yield strength.*

Confirmation of the correlation between mobile hydrogen and dislocations

To confirm the origin of the self-defined mobile H to be correlated to H trapped by dislocations, the dislocation density was modified for the Fe-C-Ti alloy B in the as-Q condition. Cold deformation of 3% was applied and the corresponding TDS spectra were analysed to verify whether the increase of dislocation density could be visualized by TDS. These tests were performed on two different TDS devices. On the one hand, the same TDS apparatus (TDS 1) as described above was used (cf. Fig. 4) requiring one hour between charging and measuring due to the necessity of a vacuum condition in the analysis chamber. On the other hand, another TDS device (TDS 2) was used where the analysis started one minute after H charging, similar as hot/melt extraction. As such, it was possible to detect mobile H and the correlation between mobile H and H trapped at dislocations could be established. These results are shown in Fig. 7.

Hardly any change was observed when the two samples with a different degree of cold deformation were tested by TDS 1. Consequently, the induced increase of dislocation density cannot be detected since H trapped at dislocations has already left the sample, which is the mobile H, as defined previously. Similar results were observed in [25]. However, when TDS 2 is used, different observations were made. At first, when considering the sample without deformation, an additional peak appeared in front of the peak observed by TDS 1. The content of this peak corresponds to the amount of mobile H, i.e. the H which was released and not detected when using TDS 1. Moreover, when the sample with cold deformation is considered in TDS 2, the first peak clearly increased, indicating that the increase in dislocation density resulted in more H trapped by the dislocations. This increase was not detected by TDS 1, confirming the correlation between the mobile H and the H trapped by dislocations.

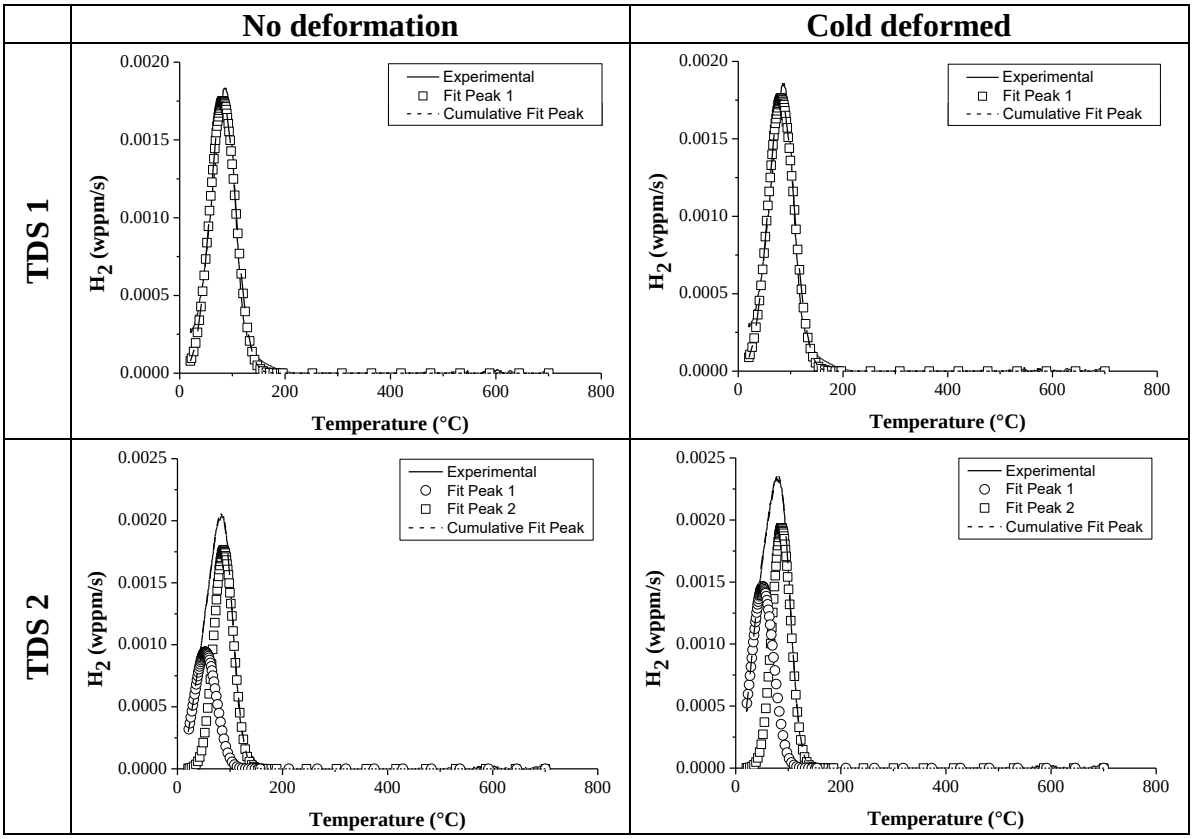

Fig. 7: *TDS spectra determined by two different TDS devices (TDS 1 and TDS 2) of the Fe-C-Ti alloy B in the as-Q condition for the not deformed and cold deformed condition.*

Conclusion

Four lab cast Fe-C-X materials (with X = Ti, Cr, Mo or V) with three different chemical compositions were investigated in both as-Q and Q&T condition. The effect of the present carbides on the H trapping and H induced mechanical degradation was evaluated. The tempered induced carbides trapped a significant amount of H as observed by TDS. The amount of mobile H, associated with H trapped at the dislocations, played a determinant role in the degree of HE. This was nicely illustrated by a correlation between the degree of HE and the amount of mobile H. The improved relation when the Fe-C-V materials were excluded from the correlation indicated the importance of an enhanced dislocation mobility in the presence of H, i.e. the HELP mechanism.

A comparative TDS analysis with two different TDS devices on not deformed and cold deformed material revealed an additional peak linked to mobile H when H saturated samples were tested one minute after charging in TDS 2. Moreover, the increase in dislocation density was detectable with TDS 2, while no variation was observed in TDS 1. This confirmed the link between mobile H and dislocations.

Acknowledgements

The authors thank the Special Research Fund (BOF), UGent (BOF15/BAS/06) and the Agency for Innovation by Science and Technology in Flanders (IWT) for support (Project nr SB111205), V. Bliznuk and E. Wallaert for the TEM images. The authors also acknowledge the technicians and staff working at the hydrogen laboratory at ArcelorMittal R&D Gent and the Department of Materials, Textiles and Chemical Engineering, UGent, for their help with the experiments and sample preparation.

References

1. M. Loidl, Adv Mat Process, **169** (2011) 22.
2. W.H. Johnson, Proc Royal Society London, **23** (1875) 168
3. A.R. Troiano, Trans ASM, **52** (1960) 54.
4. C.D. Beachem, Met Trans A, **3** (1972) 437.
5. S.P. Lynch, Scripta Mat, **61** (2009) 331.
6. S. Vervynckt, K. Verbeken, B. Lopez and J.J. Jonas, Int Mat Rev, **57** (2012) 187.
7. T. Asaoka, G. Lapasset, M. Aucouturier, P. Lacombe, Corros NACE, (1978), 39.
8. H.G. Lee, J.Y. Lee, Acta Met, **32** (1984) 131.
9. G.M. Pressouyre, I.M. Bernstein, Met Trans A, **9A** (1978) 1571.
10. F.G. Wei, T. Hara, K. Tsuzaki, Met Mat Trans B, **35B** (2004) 587.
11. F.G. Wei, K. Tsuzaki, Met Mat Trans A, **37A** (2006) 331.
12. D. Pérez Escobar, E. Wallaert, L. Duprez, A. Atrens, K. Verbeken, Met Mat Int, **19** (2013) 741.
13. H. Asahi, D. Hirakami, S. Yamasaki, ISIJ Intl, **43** (2003) 527.
14. D. Li, R.P. Gangloff, J.R. Scully, Met Mat Trans A, **35** (2004) 849.
15. G.L. Spencer, D.J. Duquette, The role of V carbide traps in reducing the HE susceptibility of high strength alloy steels, Watervliet, N.Y., (1998).
16. T. Depover, O. Monbaliu, E. Wallaert, K. Verbeken, Int Journal of H Energy, **40** (2015) 16977.
17. T.B. Hilditch, S.B. Lee, J.G. Speer, D.K. Matlock, SAE Technical Paper, (2003) http://dx.doi.org/10.4271/2003-01-0525.

18. M. Koyama, E. Akiyama, Y.K. Lee, D. Raabe, K. Tsuzaki, Int Journal of H Energy, **42** (2017) 12706.
19. T. Depover, D. Pérez Escobar, E. Wallaert, Z. Zermout, K. Verbeken, Int Journal of H Energy, **39** (2014) 4647.
20. J.A. Ronevich, J.G. Speer, D.K. Matlock, SAE Int Journal Mat Man, **3** (2010) 255.
21. M. Koyama, C. Tasan, E. Akiyama, K. Tsuzaki, D. Raabe, Acta Mat, **70** (2014) 174.
22. H. Yu, J.S. Olsen, A. Alvaro, V. Olden, J. He, Z. Zhang, Eng Fract Mech, **157** (2016) 56.
23. D. Pérez Escobar, K. Verbeken, L. Duprez, M. Verhaege, Mat Sci and Eng A, **551** (2012) 50.
24. D. Pérez Escobar, C. Miñambres, L. Duprez, K. Verbeken, M. Verhaege, Corrosion Science, **53** (2011) 3166.
25. D. Pérez Escobar, T. Depover, E. Wallaert, L. Duprez, K. Verbeken, M. Verhaege, Acta Mat, **60** (2012) 2593.
26. T. Depover, E. Wallaert, K. Verbeken, Mat Sci and Eng A, **649** (2016) 201.
27. A. Laureys, T. Depover, R. Petrov, K. Verbeken, Int Journal of H Energy, **40** (2015) 16901.
28. A. Laureys, T. Depover, R. Petrov, K. Verbeken, Materials Characterization, **112** (2016) 169.
29. F.G. Wei, T. Hara , K. Tsuzaki, "Nano-precipitates design with H trapping character in high strength steels", in Proc of the Int H Conf, Jackson, ASM Int, Jackson, WY (2008) pp. 448-455.
30. T. Depover, K. Verbeken, Mat Sci and Eng A, **669** (2016) 134.
31. T. Depover, K. Verbeken, Int Journal of H Energy, **41** (2016) 14310.
32. T. Depover, K. Verbeken, Corrosion Science, **112** (2016) 308.
33. T. Depover, K. Verbeken, Mat Sci and Eng A, **675** (2016) 299.